PHYSICAL REVIEW E **90**, 032923 (2014)

Subcritical Turing bifurcation and the morphogenesis of localized patterns

Víctor Breña-Medina[1,2,*] and Alan Champneys[2]

[1] *Departamento de Nanotecnología, Centro de Física Aplicada y Tecnología Avanzada, Universidad Nacional Autónoma de México, Juriquilla No. 3001, Querétaro 76230, Mexico*

[2] *Department of Engineering Mathematics, University of Bristol, Queen's Building, University Walk, Bristol BS8 1TR, United Kingdom*

(Received 21 January 2014; published 26 September 2014; corrected 2 October 2014)

Subcritical Turing bifurcations of reaction-diffusion systems in large domains lead to spontaneous onset of well-developed localized patterns via the homoclinic snaking mechanism. This phenomenon is shown to occur naturally when balancing source and loss effects are included in a typical reaction-diffusion system, leading to a super- to subcritical transition. Implications are discussed for a range of physical problems, arguing that subcriticality leads to naturally robust phase transitions to localized patterns.

DOI: 10.1103/PhysRevE.90.032923 PACS number(s): 82.40.Ck, 05.45.−a, 47.20.Ky, 47.54.−r

I. INTRODUCTION

Reaction-diffusion systems are known to give rise to a wide variety of stationary and oscillatory patterns; see, e.g., Refs. [1–3]. The primary mechanisms for explaining transition from quiescent to patterned states is the instability first described by Turing [4]. Such patterns are used to explain diverse physical phenomena, such as gas discharge dynamics [5], active fluid behavior [6], and tumor growth [7]. Now diffusion-driven instability, or *Turing bifurcation*, is a key part of any graduate course on nonlinear far-from-equilibrium physics or biology. For systems in large domains, however, many different wave numbers can become unstable in Turing bifurcations for nearby parameter values, and mode interactions can lead to a remarkable richness in patterns and their dynamics; see, e.g., Ref. [8].

A different explanation of *localized* pattern formation has emerged in recent years: the so-called homoclinic snaking mechanism [9,10]. The one-dimensional (1D) generalized Swift-Hohenberg equation with competing nonlinear terms is a canonical model for such analysis [11,12]. In two dimensions a richness of localized stripy, spotty, hexagonal, square-wave, and target-like patterns have been observed [13–15]. The mechanism has been shown to underlie many physical observations such as the onset of turbulent spots in plain Couette flow [16], stationary patterns in binary convection [17], and localized modes in optical cavities [18].

One of the distinctions between the homoclinic snaking and Turing bifurcation pattern formation theories is that the Swift-Hohenberg equation has variational structure, which can be linked to the free energy of the system. General systems of reaction diffusion equations for which the Turing mechanism applies do not typically have such variational structure. However, the snaking mechanism still applies to Swift-Hohenberg equations with broken variational structure [19], provided spatial reversibility is retained, although stationary asymmetric patterns are lost.

The purpose of this paper then is to show how the connection between homoclinic snaking and Turing instability analysis gives a robust explanation for the formation of localized patterns in reaction-diffusion systems. We show that this robustness arises from inclusion of source and loss terms in reaction-diffusion models, which realistic effects are often ignored in canonical models. For example, a model equivalent to the system we study below but without source and loss terms gives rise to wave pinning but no localized patterns [20]. Inclusion of such terms naturally breaks material conservation and paves the way for effective competing nonlinear terms, and in turn this allows Turing bifurcations to become *subcritical*. We show that this subcriticality is equivalent to the key condition for homoclinic snaking to occur in long domains (see also Ref. [13]). Hence, upon considering long domains, we can set the backbone conditions under which reaction-diffusion systems naturally give rise to spots and pulses, rather to than just spatially extended patterns (see also Ref. [3] for further experimental and theoretical evidence).

It is worth mentioning earlier related work of Yochelis *et al.* [21] who performed numerical bifurcation analysis on the Gierer-Meinhardt system, which includes a rational nonlinearity. They also found the existence of a bistability region and a subcritical Turing bifurcation that leads to homoclinic snaking; see also Ref. [22] for further details. The novelty of the present paper is to show that such scenarios are in some sense generic and can occur for a pure-power nonlinear system, given the presence of source and loss terms.

II. LOCAL ANALYSIS

For the ease of explanation, we shall perform our detailed calculations in one dimension in space. Extension to higher spatial dimension is in principle possible as we shall indicate in what follows, although there are additional considerations due to the range of different spatial symmetries of underlying patterns, stripes, rolls, and hexagonal lattices, among others; see Refs. [14,15,23]. We shall also apply the theory to reaction-diffusion systems with just two interacting species and a single nonlinear interaction term. Application to more complex systems is in principle straightforward because the theory is built upon the principle of normal-form reduction.

Consider a reaction-diffusion system

$$U_t = D_1 U_{xx} + F(U,V;\mu), \tag{1a}$$

$$V_t = D_2 V_{xx} + G(U,V;\mu), \tag{1b}$$

*victor.brena@bristol.ac.uk; Present address: Centro de Ciencias Matemáticas, Universidad Nacional Autónoma de México Campus Morelia, México.

for $x \in (-L/2, L/2)$, subject to homogeneous Neumann boundary conditions. Here parameters D_1 and D_2 are diffusion coefficients and F and G are sufficiently smooth functions. Without loss of generality time scales have been scaled to unity, but the length scale L is retained.

The linear analysis provides of the usual conditions under which Turing bifurcations occur; see Ref. [2]. Thus, suppose there exists an isolated homogeneous equilibrium $(U,V)^T = (U_0,V_0)^T$. Upon substituting the incremental variables $U = U_0 + u$ and $V = V_0 + v$ into system (1), we obtain

$$\begin{pmatrix} u_t \\ v_t \end{pmatrix} = \begin{pmatrix} D_1 u_{xx} \\ D_2 v_{xx} \end{pmatrix} + \mathbf{A}(\mu)\begin{pmatrix} u \\ v \end{pmatrix} + \begin{pmatrix} f(u,v;\mu) \\ g(u,v;\mu) \end{pmatrix}, \tag{2}$$

where $\mathbf{A} = \{a_{ij}\}$ with $a_{11}(\mu) = F_U$, $a_{12}(\mu) = F_V$, $a_{21}(\mu) = G_U$, $a_{22}(\mu) = G_V$ evaluated at the steady state, and f and g gather all remaining higher-order terms. Under the usual assumptions of Turing bifurcation analysis, we first need to assume that the homogeneous steady state is stable in the absence of diffusion; that is, trace $\mathbf{A} < 0$ and $\det \mathbf{A} > 0$.

To find diffusion-driven instability with spatial wave number κ we look for modes of the form

$$\cos(\kappa(x - L/2))\begin{pmatrix} C_1 \\ C_2 \end{pmatrix}, \quad C_1^2 + C_2^2 > 0, \tag{3}$$

where $\kappa = \kappa_m = m\pi/L$ for some positive integer mode number m. This leads to the search for zero eigenvalues λ of the matrix

$$\mathbf{A}_\kappa(\mu) = \begin{pmatrix} a_{11} - D_1\kappa^2 & a_{12} \\ a_{21} & a_{22} - D_2\kappa^2 \end{pmatrix}, \tag{4}$$

with wave number $\kappa = \sqrt{(D_2 a_{11} + D_1 a_{22})/(D_1 D_1)}$. The condition for instability is that κ is real, which is guaranteed for a stable equilibrium [with sign $(a_{11}a_{22}) < 0$] if $D_1 D_2 \ll \max\{D_1^2, D_2^2\}$. Without loss of generality, suppose $a_{22} < 0$ and that $D_1 \ll D_2$, which, in comparison to the V component, implies that the U component diffuses slowly.

We now perform a proper comparison between the two theories in question, in the case of a long domain $L \gg 1$. We suppose that at parameter value $\mu = \mu_c$ there is a double zero eigenvalue of A_κ, corresponding to a large mode number m_c, not necessarily an integer. The condition for such a double root is

$$(D_2 a_{11} + D_1 a_{22})^2 = 4 D_1 D_2 \det \mathbf{A}. \tag{5}$$

On the one hand, for a $L \gg 1$ there will be a large number of Turing bifurcations for nearby κ values corresponding to $\kappa = m\pi/L$ for integers m close to m_c. Generically, μ will depend quadratically on κ close to μ_c, which would imply a double accumulation of Turing bifurcations: one family corresponding to higher wave numbers $\kappa > \kappa_c$, the other to lower wave numbers $\kappa < \kappa_c$; see in Fig. 1(a) the mode numbers m which correspond to zeros of the dispersion relation as μ tends towards μ_c.

Alternatively, in the limit $L \to \infty$, so-called spatial dynamics can be applied (see, e.g., Ref. [9]) where steady states $(U(x,t),V(x,t))^T = (u(x),v(x))^T$ of (1) are sought by considering the ODE system on the real line

$$D_1 u_{xx} + F(u,v;\mu) = 0\,, \quad D_2 v_{xx} + G(u,v;\mu) = 0\,,$$

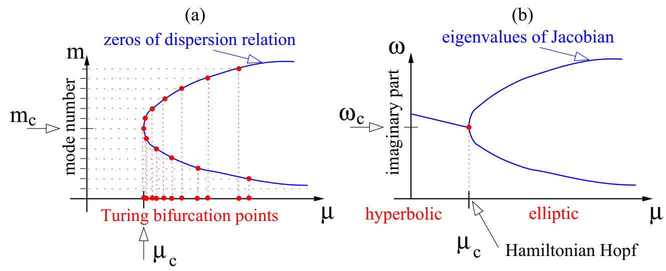

FIG. 1. (Color online) The equivalence between (a) the mode numbers accumulation point of Turing bifurcations and (b) a Hamiltonian-Hopf bifurcation point for long domains.

as a four-dimensional dynamical system in "time" x. As such, the symmetry $(u_x,v_x)^T \to (-u_x,-v_x)^T$ and $x \to -x$ corresponds to a spatial reversibility. In this context, a homogeneous steady state $(U_0,V_0)^T$ of the PDE corresponds to an equilibrium $(u,u_x,v,v_x)^T = (U_0,0,V_0,0)^T$ within the fixed point set of the reversibility. The linearization of the system about such an equilibrium would take the form

$$\begin{pmatrix} u_{xx} \\ v_{xx} \end{pmatrix} + \begin{pmatrix} a_{11}/D_1 & a_{12}/D_1 \\ a_{21}/D_2 & a_{22}/D_2 \end{pmatrix}\begin{pmatrix} u \\ v \end{pmatrix} = \begin{pmatrix} 0 \\ 0 \end{pmatrix}. \tag{6}$$

Such an equilibrium will undergo a transition from being hyperbolic to elliptic at a Hamiltonian-Hopf bifurcation (also known as a reversible 1:1 resonance) [24], which occurs, under suitable nondegeneracy conditions, when there is a double pair of complex conjugate eigenvalues $\pm i\omega$ of the Jacobian in (6). Upon substituting $(u,v)^T = (A,B)^T \exp(i\omega x)$ into (6), we find that we need a double root to

$$D_1 D_2 \omega^4 - (D_2 a_{11} + D_1 a_{22})\omega^2 + \det \mathbf{A} = 0,$$

which leads to precisely the same condition for a fold Turing points with respect to κ, namely, equality as in (5); see Fig. 1(b). It is straightforward to show that the condition for a criticality of the Turing bifurcation at the double root is precisely the same as the condition for the criticality of the corresponding Hamiltonian-Hopf; see, e.g., Ref. [25]. Both problems may be expressed as via an amplitude equation whose real part reads [24]

$$Z''(\xi) = q_1(\mu - \mu_c)Z + q_3 Z|Z|^2 + q_5 Z|Z|^4\,. \tag{7}$$

A key prediction of the homoclinic snaking mechanism [10] is the birth of a spatially localized mode (a homoclinic orbit in space x) if the Hamiltonian-Hopf bifurcation is subcritical, $q_1 q_3 > 0$. For small $q_1 q_3 > 0$, then, provided $q_1 q_5 < 0$, an unfolding of the normal form shows that there is a heteroclinic connection from a background state to a nontrivial periodic orbit. Taking account of beyond-all-orders terms in the normal form [26,27] enables an analysis to be undertaken in which we find infinitely many homoclinic orbits arranged on two closed curves; see Fig. 3(b) below.

III. ILLUSTRATION FOR A GENERALIZED SCHNAKENBERG SYSTEM

In order to illustrate our findings, we here consider the generalized Schnakenberg system, which is a spatially homogeneous form of a model proposed in Ref. [28] of pattern formation via interaction between active U and inactive V small G-proteins in subcellular-level biological morphogenesis:

$$U_t = D_1\nabla^2 U + k_2U^2V - (c+r)U + hV, \quad (8a)$$

$$V_t = D_2\nabla^2 V - k_2U^2V + cU - hV + b, \quad (8b)$$

in which all parameters are taken to be positive. Here the model models a nonreversible autocatalytic process and differs from the standard Schnakenberg and Gray-Scott systems through the presence of a production term b of the inactive component and removal rate r of the activated component. Notice that, as can easily be shown, otherwise Turing bifurcations are always supercritical in straightforward Schnakenberg and Gray-Scott systems.

There is a unique homogeneous equilibrium

$$U_0 \equiv \frac{b}{r}, \quad V_0 \equiv \frac{br(c+r)}{k_2b^2 + hr^2}. \quad (9)$$

Upon substituting the incremental variables $U = U_0 + u$ and $V = V_0 + v$ into system (8) in 1D, we get a system of the form (2) where the coefficients of $\mathbf{A}$ are given by

$$a_{11} = \frac{(c+r)(k_2b^2 - hr^2)}{k_2b^2 + hr^2}, \quad (10a)$$

$$a_{12} = -a_{22} = \frac{k_2b^2 + hr^2}{r^2}, \quad (10b)$$

$$a_{21} = \frac{chr^2 - k_2b^2(c+2r)}{k_2b^2 + hr^2}, \quad (10c)$$

and the nonlinear terms

$$\begin{pmatrix} f \\ g \end{pmatrix} \equiv k_2(u^2v + V_0u^2 + 2U_0uv)\begin{pmatrix} 1 \\ -1 \end{pmatrix}. \quad (11)$$

Note that the nonlinearity contains both quadratic and cubic terms when written in these coordinates. It is straightforward to show that the steady state $(U_0, V_0)^T$ is asymptotically stable in the absence of diffusion provided $c + r < 8h$.

Figure 2(a) shows the dispersion relation as function of squared wave number κ_m^2, for several values of a bifurcation parameter k_2. In this and unless otherwise stated in what follows we use parameter values $k_2 \in (0,5)$ and $b = 1$, $c = 1$, $r = 1$, $h = 1$, $D_1 = 0.1$, $D_2 = 10$.

To calculate the criticality condition of the Turing instabilities of (8), we follow a Lyapunov-Schmidt reduction method [29]. Upon obtaining the steady-state smooth functional $\boldsymbol{\phi} = \boldsymbol{\phi}(U,V,\mu)$, which comes from setting u_t and v_t to zero, and hence defining the bifurcation function $g(z,\mu) \equiv \langle \mathbf{w}^*, \boldsymbol{\phi}(z\mathbf{w},\mu)\rangle$ at the steady state $\mathbf{w} = (u - U_0, v - V_0)^T$, the result is a so-called *bifurcation equation* $g = 0$, the leading-order expansion of which can be written

$$g(z,\mu) = q_1\mu z + q_3z^3 + q_5z^5 + O(\mu^2 z, \mu z^3). \quad (12)$$

Note that the form of g is identical to the right-hand side of the amplitude equation (7). The bifurcation parameter here is defined as $\mu = k_2 - k_{2c}$ and the scalar variable z parametrizes the amplitude of the component of the Turing pattern in the kernel of the matrix $\mathbf{A}_\kappa(\mu) = -\mathbf{D}\kappa^2 + \mathbf{A}$, where $\mathbf{D}$ is the diffusivity matrix. The calculation of the coefficients q_i is

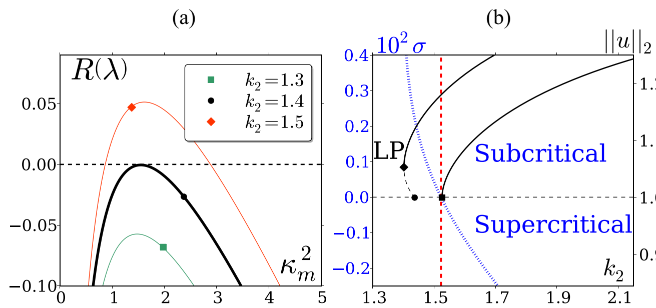

FIG. 2. (Color online) (a) Dispersion relation of $\mathbf{A}_\kappa(\mu)$ restricted to the eigenspace spanned by modes of the form (3). The bold solid curve corresponds to where a double root of det $[\mathbf{A}_\kappa(\mu)] = 0$ occurs. (b) Bifurcation diagram and pitchfork criticality condition; stable branches are shown as solid lines, the filled circle at $k_2 = 1.4369$ corresponds to a subcritical bifurcation, and the square at $k_2 = 1.5258$ to a supercritical bifurcation. The subcritical branch undergoes to a fold bifurcation (LP). The pitchfork criticality condition is depicted as a (blue) heavily dashed line, where the criticality transition is indicated by a (red) vertical dashed line at $k_2 = 1.5226$.

straightforward but lengthy, and full details are available in Ref. [30]; we omit the details for brevity.

Note that such a bifurcation equation (12) can be derived in principle in a higher dimensional spatial domain Ω. There a vector reduced bifurcation function $\mathbf{g}$ can be computed by projecting onto the eigenspace defined by modes satisfying the boundary value problem

$$\nabla^2\mathbf{w} + |\boldsymbol{\kappa}|^2\mathbf{w} = \mathbf{0}, \quad (\mathbf{n}\cdot\nabla)\,\mathbf{w}|_{\partial\Omega} = \mathbf{0}.$$

In computing the scalar function g, we find that trivially $g_\mu(0,0) = 0$ and $g_{\mu\mu}(0,0) = 0$, by virtue of the equilibrium being at the origin and having a zero eigenvalue. Also, owing to the reflection symmetry in x, the reduced bifurcation function must be odd in z, despite the presence of quadratic terms in the original equation.

In the parameter region under investigation the sub- or supercriticality of the pitchfork (Hamiltonian-Hopf) bifurcation is determined by the sign of

$$\sigma = q_1q_3;$$

see Ref. [24]. Figure 2(b) plots σ, as a function of k_2 close to k_{2c}. We have also checked that q_1q_5 is negative in all the entire parameter region of interest. The figure also shows computed bifurcating branches close to the point where σ changes sign, where we can see a restabilizing fold (limit point) in the case of the subcritical bifurcation.

Now consider variation of a second parameter. For convenience we choose D_1. Figure 3(a) depicts a two-parameter bifurcation diagram showing the Hamiltonian-Hopf bifurcation curve, the codimension-two point at which $\sigma = 0$ and the numerically computed "snaking region" in which localized states exist in the (k_2, D_1) plane. In accordance with the usual analysis of homoclinic snaking, inside this region there are two branches of localized states. The states are all invariant under the reversibility, and at each fold the number of pulses varies, so that each second successive horizontal-like branch has two additional large pulses. We remark that, in contrast to the Swift-Hohenberg equation for example, there

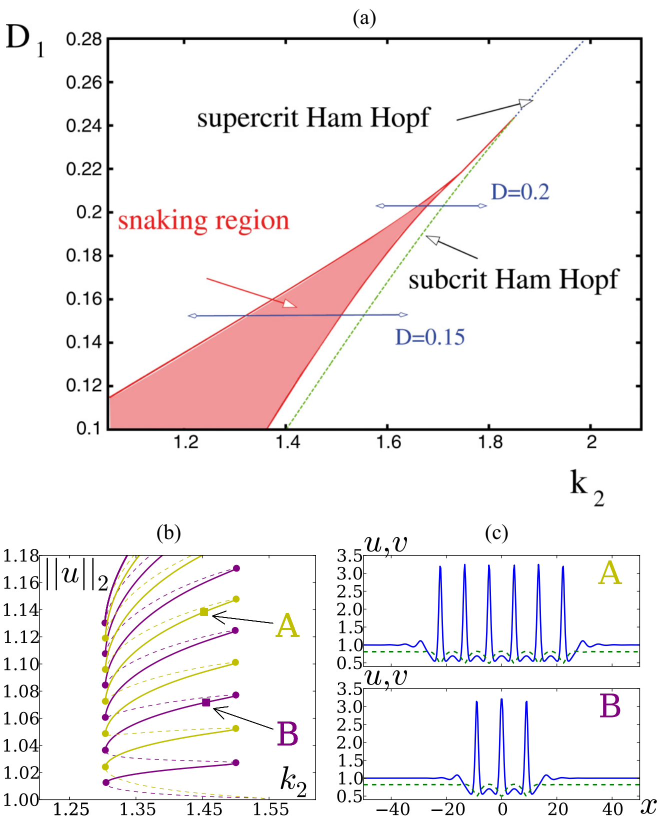

FIG. 3. (Color online) (a) The snaking region (shaded) inside which homoclinic snaking is observed in the (k_2,D_1) parameter plane. (b) Homoclinic snaking; even-solutions branch (yellow) and odd-solutions branch (purple), and fold bifurcations (filled circles); bold solid lines indicate stable branches; $D_1 = 0.15$. (c) Samples of multipulse homoclinic stable solutions on the even and odd branch for $k_2 = 1.45$, top and bottom panels, respectively, which correspond to six-spike solution (label A) and three-spike solution (label B) in panel (b). The u component (solid line) and v component (dashed line) are plotted for a domain size $L = 100$.

is no variational structure in the system (8), which therefore implies there are no asymmetric stationary localized states (so-called "ladders" in a "snakes and ladders" bifurcation diagram).

In addition, we have computed stability of the states shown in Fig. 3(b) using a standard three-point uniform finite differences method and an eigenvalue solver. We have numerically found that stable branches occur similarly to results previously found for the Swift-Hohenberg system (e.g., Refs. [12,19]) as is shown (solid lines) in Fig. 3(b). There stable branches lose stability in a fold bifurcation (filled circles) where branches of solutions with odd and even numbers of spikes annihilate each other. Examples of stable solutions are shown in Fig. 3(c); note that number of spikes correspond to ladder step.

IV. 2D SIMULATION RESULTS

To illustrate that a similar localized pattern formation mechanism is likely to apply in higher spatial dimensions we have performed simulations of the same system (8), on a large square domain with $L_{x,y} = 300$. Specifically we have used a finite difference method implemented in Matlab, with spatial resolution 300×300. The computations were run a long time until steady state reached. The results are presented in Fig. 4.

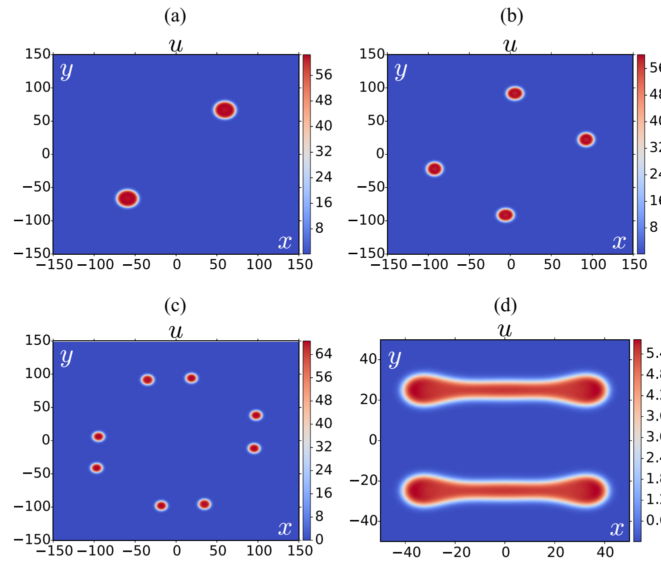

FIG. 4. (Color online) Stable patterns for a two-dimensional square domain $L_{x,y} = 300$ on a cool-warm scale (side bar). Localized (a) two-spot for $r = b = 10^{-4}$, $k_2 = 4 \times 10^{-3}$, and $D_1 = 0.13$, (b) four-spot for $r = b = 5 \times 10^{-4}$, (c) eight-spot for $D_1 = 0.11$, and other parameter values as in (a); (d) two-stripe: $r = b = 10^{-4}$, $k_2 = 0.6$, $D_1 = 0.1$, and $L_{x,y} = 100$. Other parameter values: $c = 0.1$, $h = 10^{-2}$, and $D_2 = 10$.

We have found a collection of different localized patterns under the conditions of equal source and loss terms $b = r$. Samples of these can be seen in Figs. 4(a)–4(c). Taking similar initial conditions that was a 10^{-2} perturbation from the homogeneous equilibrium (9) resulted in the two-spot pattern depicted in Fig. 4(a). Taking this solution as an initial conditions, a slight increase in b and r resulted in the localized four-spot pattern depicted in Fig. 4(b). The dynamics of this process was such that each spot arises through a form of spot-splitting dynamics [31]. In a similar fashion, we slightly decreased D_1 instead. In so doing, a localized eight-spot pattern is obtained from the four-spot pattern; see Fig. 4(c).

In addition, we also noted that upon performing a similar computation but changing $b = r$ or D_1 in the other directions results in a either a completely different form of spatially extended pattern or no pattern at all. This suggests that hysteretic behavior is taking place, which should be a consequence of an overlapping structure of stable branches similar to Fig. 3(b).

These patterns, however, are just a few examples of the spotlike patterns that we were able to find and indicate that the mechanism we have identified is likely to be robust in higher dimensions. A full exploration in the spirit of Refs. [13–15] though is left for future work. It is interesting to note though that we were unable to find any localized patterns for $b \neq r$. This suggests that well-balanced source and loss plays an important role in the (nonvariational) pattern formation mechanism under investigation in higher dimensions.

On the other hand, in Fig. 4(d), a stripelike pattern is depicted. We initially obtained a two-spot pattern as before in a smaller domain, and it was taken as an initial condition for a second run. In so doing, note that upon significantly increasing k_2 and slightly decreasing D_1 parameter values the two-spot pattern dramatically changes. Moreover, upon taking this solution as an initial condition once again but in a much larger domain, a pattern consisting of spots and stripes emerges (not shown). Patterns as such have been observed in nonhomogeneous domains; see Refs. [32,33]. A further analysis is nevertheless also left for future work.

V. CONCLUSIONS

In summary, we have shown that canonical reaction-diffusion systems can generate localized patterns spontaneously, which, close to a relevant codimension-two point, can occur at small amplitude. In particular, taking realistic source and loss terms into account can provide conditions for a subcritical Turing bifurcation to occur. Taking the paradigm of spatial dynamics, on a long domain, the Turing bifurcation corresponds to where two complex eigenvalues collide on the imaginary axis (a Hamiltonian-Hopf bifurcation). In the presence of spatial reversibility, this provides exactly the right ingredients for the spontaneous formation of localized patterns through the so-called homoclinic snaking mechanism. Note that any realistic physical, chemical or biological systems, especially those found in nature, are likely to feature such source and loss terms.

Moreover, as argued more carefully in Ref. [34] this method of pattern formation is likely to be more robust than via the more traditional supercritical Turing instability, and hence to be chosen by nature. In the supercritical case, the pattern is always spatially extended, is born from zero amplitude and, in long domains is typically subject to further instabilities through mode interactions. In contrast for the subcritical Turing bifurcations investigated here, we find jumps to well-formed, finite amplitude patterns that are localized in the spatial domain. Due to the hysteretic nature of fold bifurcations seen in the snaking bifurcation branch, small fluctuations in parameter values or small stochastic perturbations of the kinetics would not typically destroy the localized pattern. In addition, the presence of a weak spatial inhomogeneity will result in bifurcation diagram similar to that in Fig. 3(b), but slanted so that the folds of the snake occur at different values (results not shown). For example, Ref. [34] considers the system (8), in a different parameter regime, in a long (but finite) domain in one dimension with a spatial gradient multiplying the bifurcation parameter k_2. The result is reminiscent of a finite portion of a slanted snake bifurcation diagram where the patterns with a higher number of spots occur for higher k_2 values. This can be explained using the concept of *slanted snaking* established by Dawes [35], where in this case the spatial gradient is replaced by a scalar field that is neutrally stable. We therefore believe the mechanism we have uncovered will prove important in explaining and predicting observations of localized patterns in certain a wide variety of physical systems (see, for example, Ref. [3]) and will only be accentuated by spatial homogeneity.

ACKNOWLEDGMENT

We thank to Arik Yochelis for his valuable comments. The research of V. F. B.-M. was supported by CONACyT Grant No. 167244.

[1] S. Kondo and T. Miura, Science **329**, 1616 (2010).
[2] J. D. Murray, *Mathematical Biology II: Spatial Models and Biomedical Applications*, 3rd ed. (Springer-Verlag, New York, 2002).
[3] V. K. Vanag and I. R. Epstein, Chaos **17**, 037110 (2007).
[4] A. M. Turing, Phil. Trans. Roy. Soc. Lond. B **237**, 37 (1952).
[5] H. G. Purwins, H. U. Boedeker, and Sh. Amiranashvili, Adv. Phys. **59**, 485 (2010).
[6] J. S. Bois, F. Julicher, and S. W. Grill, Phys. Rev. Lett. **106**, 028103 (2011).
[7] E. Khain and L. M. Sander, Phys. Rev. Lett. **96**, 188103 (2006).
[8] R. Hoyle, *Pattern Formation: An Introduction to Methods* (Cambridge University Press, Cambridge, 2006).
[9] M. Beck, J. Knobloch, D. J. B. Lloyd, B. Sandstede, and T. Wagenknecht, SIAM J. Math. Anal. **41**, 936 (2009).
[10] P. D. Woods and A. R. Champneys, Physica D **129**, 147 (1999).
[11] J. Burke and E. Knobloch, Phys. Rev. E **73**, 056211 (2006).
[12] J. Burke and E. Knobloch, Chaos **17**, 037102 (2007).
[13] D. Avitabile, D. J. B. Lloyd, J. Burke, E. Knobloch, and B. Sandstede, SIAM J. Appl. Dyn. Syst. **9**, 704 (2010).
[14] D. J. B. Lloyd, B. Sandstede, D. Avitabile, and A. R. Champneys, SIAM J. Appl. Dyn. Syst. **7**, 1049 (2008).
[15] D. J. B. Lloyd and B. Sandstede, Nonlinearity **22**, 485 (2009).
[16] T. M. Schneider, J. F. Gibson, and J. Burke, Phys. Rev. Lett. **104**, 104501 (2010).
[17] C. Beaume, A. Bergeon, and E. Knobloch, Phys. Fluids **23**, 094102 (2011).
[18] D. Gomila, P. Colet, M. S. Miguel, A. J. Scroggie, and G.-L. Oppo, IEEE J. Quantum Electronics **39**, 238 (2003).
[19] S. M. Houghton and E. Knobloch, Phys. Rev. E **84**, 016204 (2011).
[20] Y. Mori, A. Jilkine, and L. Edelstein-Keshet, SIAM J. Appl. Math. **71**, 1402 (2011).
[21] A. Yochelis, Y. Tintut, L. L. Demer, and A. Garfinkel, New J. Phys. **10**, 055002 (2008).
[22] A. Yochelis and A. Garfinkel, Phys. Rev. E **77**, 035204(R) (2008).
[23] D. J. B. Lloyd and H. O'Farrell, Physica D **253**, 23 (2013).
[24] G. Iooss and M.-C. Perouème, J. Diff. Eqns. **102**, 62 (1993).
[25] J. Burke and E. Knobloch, Discrete Continuous Dyn. Syst. Supp. **170**, 170 (2007).
[26] A. D. Dean, P. C. Matthews, S. M. Cox, and J. R. King, Nonlinearity **24**, 3323 (2011).
[27] G. Kozyreff and S. J. Chapman, Phys. Rev. Lett. **97**, 044502 (2006).

[28] R. J. H. Payne and C. S. Grierson, PLoS ONE **4**, e8337 (2009).

[29] M. Golubitsky and D. Schaeffer, *Singularities and Groups in Bifurcation Theory*, Vol. 1 (Springer, New York, 1985).

[30] V. F. Breña-Medina, PhD. thesis, University of Bristol, 2013.

[31] Y. Nishiura and D. Ueyama, Physica D **130**, 73 (1999).

[32] V. Brena-Medina, D. Avitabile, A. R. Champneys, and M. J. Ward, arXiv:1403.5318 [nlin.PS].

[33] R. G. Plaza, F. Sánchez-Garduño, P. Padilla, R. A. Barrio, and P. K. Maini, J. Dyn. Diff. Equ. **16**, 1093 (2004).

[34] V. Breña-Medina, A. R. Champneys, C. Grierson, and M. J. Ward, SIAM J. Appl. Dyn. Syst. **13**, 210 (2014).

[35] J. H. P. Dawes, SIAM J. Appl. Dyn. Syst. **7**, 186 (2008).